

# Performance Characterization of a Real-Time Massive MIMO System with LOS Mobile Channels

Paul Harris, *Student Member, IEEE*, Steffen Malkowsky, *Student Member, IEEE*, Joao Vieira, Erik Bengtsson, Fredrik Tufvesson, *Fellow, IEEE*, Wael Boukley Hasan, *Student Member, IEEE*, Liang Liu, *Member, IEEE*, Mark Beach, *Member, IEEE*, Simon Armour, and Ove Edfors, *Member, IEEE*

**Abstract**—The first measured results for massive multiple-input, multiple-output (MIMO) performance in a line-of-sight (LOS) scenario with moderate mobility are presented, with eight users served in real-time using a 100-antenna base Station (BS) at 3.7 GHz. When such a large number of channels dynamically change, the inherent propagation and processing delay has a critical relationship with the rate of change, as the use of outdated channel information can result in severe detection and precoding inaccuracies. For the downlink (DL) in particular, a time division duplex (TDD) configuration synonymous with massive MIMO deployments could mean only the uplink (UL) is usable in extreme cases. Therefore, it is of great interest to investigate the impact of mobility on massive MIMO performance and consider ways to combat the potential limitations. In a mobile scenario with moving cars and pedestrians, the massive MIMO channel is sampled across many points in space to build a picture of the overall user orthogonality, and the impact of both azimuth and elevation array configurations are considered. Temporal analysis is also conducted for vehicles moving up to 29 km/h and real-time bit error rates (BERs) for both the UL and DL without power control are presented. For a 100-antenna system, it is found that the channel state information (CSI) update rate requirement may increase by 7 times when compared to an 8-antenna system, whilst the power control update rate could be decreased by at least 5 times relative to a single antenna system.

**Index Terms**—Massive MIMO, 5G, Testbed, Field Trial, Mobility

## I. INTRODUCTION

MASSIVE multiple-input, multiple-output (MIMO) has established itself as a key 5G technology that could drastically enhance the capacity of sub-6 GHz communications in future wireless networks. By taking the multi-user (MU) MIMO concept and introducing additional degrees of freedom in the spatial domain, the multiplexing performance and reliability of such systems can be greatly enhanced, allowing many tens of users to be served more effectively in the same time-frequency resource [1]. With a plethora of antennas, the law of large numbers averages out the effects of fast-fading (known as ‘channel hardening’), noise and hardware imperfections, and also makes such a system extremely robust to antenna or full radio frequency (RF) chain failures [2] [3].

In addition to theoretical work and results such as those documented in [1], [2] and [4], various institutions from

around the world have been developing large-scale test systems in order to validate theory and test algorithms with real data. Rice University presented a 96-antenna time division duplex (TDD) system in 2012 based upon the Wireless Open-Access Research Platform (WARP) platform named ARGOS, reporting some cell capacity predictions made by measuring signal to interference plus noise ratio (SINR) [5] [6]. Around the same time in Australia, the frequency division duplex (FDD) Ngarra demonstrator [7] was reported to have achieved a coded uplink (UL) spectral efficiency of 67.26 bits/s/Hz in a lab environment at 638 MHz using practical low-cost hardware. Aligning more closely with the long-term evolution (LTE) standards, Samsung published their work on Full Dimension MIMO (FD-MIMO) in [8] and [9]. This is a massive MIMO prototype that utilises a 2D antenna array form factor for deployment feasibility and cell average throughput gains of up to 3.6 have been indicated in system-level simulations. Also exploiting the elevation dimension more aggressively, ZTE reported a field trial of a TDD massive MIMO prototype in [10] where 64 transceiver units served 8 TDD-LTE commercial handsets located at different floor levels in a high-rise building, achieving a 300 Mb/s sum rate in 20 MHz of bandwidth (BW). Furthermore, their recent announcements at mobile world congress (MWC) indicate significant progress is being made in pre-5G commercial deployments with China Mobile. Coming from a slightly different perspective than the cellular providers, Facebook have developed a 96-antenna massive MIMO proof-of-concept (POC) within their Connectivity Lab capable of supporting 24 MIMO streams. They aim to conclusively demonstrate that massive MIMO could provide long-range rural connectivity from city centres and indicated a lab-based achievement of 71 bits/s/Hz in [11].

Finally, Lund University and the University of Bristol have developed 100-antenna and 128-antenna real-time testbeds capable of serving 12 wireless devices in the same time-frequency resource with a TDD LTE-like physical layer. The development of these systems underpins the work presented here. Lund University first described their 100-antenna testbed in [12] along with a distributed field-programmable gate array (FPGA) processing architecture and were the first to present such a system with real-time operation. The University of Bristol through the joint venture Bristol Is Open (BIO) [13] constructed their system the following year and worked jointly with Lund University and National Instruments (NI) to implement and test a new, centralised MIMO processing architecture, which allowed for greater flexibility in ongoing

P. Harris, W.B. Hassan, M.A. Beach and S. Armour are with the Communication Systems & Networks (CSN) Group at the University of Bristol, U.K.

S. Malkowsky, J. Vieira, E. Bengtsson, F. Tufvesson, L. Liu and O. Edfors are with the Dept. of Electrical and Information Technology, Lund University, Sweden.

development. Further details on the new architecture can be found in [14]. In 2016, two indoor trials were conducted within an atrium at the University of Bristol, and it was shown that spectral efficiencies of 79.4 bits/s/Hz and subsequently 145.6 bits/s/Hz could be achieved whilst serving up to 22 user clients [15] [16]. These spectral efficiency results are currently world records and indicate the potential massive MIMO has as a technology.

However, wireless technology is usually applied in scenarios that will involve some form of mobility, and it is therefore of great interest to investigate the evolution of massive MIMO under more dynamic channel conditions. The aforementioned measurement trials have not yet considered the progression of a composite massive MIMO channel with mobility, but measured static terminals. In [17], the authors discuss some of the potential issues with channel ageing in a macro-cell massive MIMO deployment and propose a novel ultra-dense network (UDN) approach for comparison. From simulation results, they illustrate that massive MIMO performance could significantly worsen with mobile speeds of just 10 km/h, and that the sensitivity of zero-forcing (ZF) to channel state information (CSI) errors could make matched filtering (MF) the more viable option. In [18] and [19], the theoretical impact of channel ageing on the UL and downlink (DL) performance of massive MIMO is evaluated. Interestingly, the analysis shows that a large number of antennas is to be preferred for maximum performance, even under time-varying conditions, and that Doppler effects dominate over phase noise.

In this paper, 8 user equipments (UEs) are served by a 100-antenna base Station (BS) in real-time and the first measured results for massive MIMO under moderate mobility in line-of-sight (LOS) are presented. With a large set of spatial samples taken across a mobile scenario, the singular value spread (SVS) is analysed and insight is provided on the impact of azimuth and elevation dominant array configurations. Furthermore, by measuring the full MIMO channel at a time resolution of 5 ms, temporal analysis in the form of time correlation, inter-user interference (IUI) and channel hardening is conducted for speeds up to 29 km/h. Finally, real-time bit error rates (BERs) measured for the UL and DL with no power control are presented to provide an indication of the raw performance achieved by the system.

The outline of the remainder of the paper is as follows. Sec. II provides an overview of the testbed and the additional functionality that was implemented to enable meaningful mobility measurements to be made. One measurement scenario is then outlined in Sec. III for both a static and mobile case; SVS, temporal and BER results are presented in Sec. IV; and the paper concludes with Sec. V.

## II. SYSTEM DESCRIPTION

The Lund University massive MIMO BS pictured in Fig. 1 consists of 50 NI universal software radio peripherals (USRPs), which are dual-channel software-defined radios (SDRs) with reconfigurable FPGAs connected to the RF front ends [20]. Collectively, these provide 100 RF chains, with a further 6 USRPs acting as 12 single-antenna UEs. It runs with a TDD

TABLE I  
SYSTEM PARAMETERS

Parameter	Value
# of BS Antennas	100
# of UEs	12
Carrier Frequency	1.2-6 GHz (3.7 GHz used)
Bandwidth	20 MHz
Sampling Frequency	30.72 MS/s
Subcarrier Spacing	15 kHz
# of Subcarriers	2048
# of Occupied Subcarriers	1200
Frame duration	10 ms
Subframe duration	1 ms
Slot duration	0.5 ms
TDD periodicity	1 slot

LTE-like physical layer (PHY) and the key system parameters can be seen in Table I. Using the same peripheral component interconnect express (PCIe) eXtensions for instrumentation (PXIe) platform that powers the 128-antenna system, all the remote radio heads (RRHs) and MIMO FPGA co-processors are linked together by a dense network of gen 3 PCIe fabric, and all software and FPGA behaviour is programmed via LabVIEW. A description of the Lund University system along with a general discussion of massive MIMO implementation issues can be found in [14]. The reciprocity calibration approach designed at Lund University and applied in these experiments is detailed in [21]. Further detail about the current system architecture and the implementation of a wide data-path Minimum Mean Square Error (MMSE) encoder/decoder can be found in [15], [16] and [22].

### A. Antenna Array

The Lund antenna array in Fig. 1 consists of half-wavelength spaced 3.7 GHz patch-antennas each with horizontal and vertical polarization options. For the results reported here, the 4x25 azimuth dominated portion highlighted in the image was used, with alternating horizontal and vertical polarizations across the array.

### B. Channel Acquisition

The system is defined as having  $M$  antennas,  $K$  users and  $N$  frequency domain resource blocks of size  $R_b$ . For this paper, we specifically define resource block to refer to a grouping of 12 Orthogonal Frequency Division Multiplexing (OFDM) subcarriers, with each 1200 subcarrier OFDM symbol consisting of 100 resource blocks. The estimate of the UL for each 12 subcarrier resource block  $r$  is found as

$$\mathbf{H}_r = \mathbf{Y}_r \mathbf{P}_r^* \quad (1)$$

where  $\mathbf{H}_r$  is the  $M \times K$  channel matrix,  $\mathbf{Y}_r$  is the  $M \times R_b$  receive matrix and  $\mathbf{P}_r^*$  is the diagonal  $R_b \times K$  conjugate uplink pilot matrix. Each UE sends an UL pilot for each resource block on a subcarrier orthogonal to all other users and the BS performs least-square channel estimation. Since all pilots



Fig. 1. Lund Massive MIMO Basestation with 4x25 array configuration highlighted

have a power of 1,  $\mathbf{Y}_r \mathbf{P}_r^*$  can be used rather than  $\mathbf{Y}_r / \mathbf{P}_r^*$ . All MIMO processing in the system is distributed across 4 Kintex 7 FPGA co-processors, each processing 300 of the 1200 subcarriers. In order to study the channel dynamics under increased levels of mobility, a high time resolution is desired during the capture process, which equates to a high rate of data to write to disk. To address this, a streaming process was implemented that uses the on-board dynamic random access memory (DRAM) to buffer the raw UL subcarriers.  $\mathbf{Y}_r$  is recorded in real-time to the DRAM at the measurement rate,  $T_{\text{meas}} = 5$  ms, and this data is then siphoned off to disk at a slower rate. Using this process with 2 GB of DRAM per MIMO processor, we were able to capture the full composite channel for all resource blocks a 5 ms resolution for 65 s.

The channel was sampled at least once every half-wavelength distance in space to give an accurate representation of the environment. The maximum permissible speed of mobility,  $v_{\text{max}}$ , is thus given by

$$v_{\text{max}} = \frac{\lambda}{2T_{\text{meas}}} \quad (2)$$

This results in a maximum speed of 8.1 m/s or approximately 29 km/h for temporal analysis of the channel data. For the SVS results, this constraint does not apply as the aim is to simply provide a large spatial sample set. It should also be noted that the testbed estimates the full channel every 0.5 ms (1 time slot) for real-time operation, so the speed limitation is also not applicable for the real-time BERs.

### C. Post-Processing

1) *SVS*: The SVS is one of the most powerful ways to evaluate the joint orthogonality of the user channel vectors in a MIMO system [23]. Our  $M \times K$  channel matrix for one resource block  $r$  can be described in terms of its singular value decomposition (SVD) [24] as

$$\mathbf{H}_r = \mathbf{U}_r \mathbf{\Sigma}_r \mathbf{V}_r^H \quad (3)$$

where  $\mathbf{U}_r$  and  $\mathbf{V}_r$  represent the left and right unitary matrices, and  $\mathbf{\Sigma}_r$  is the  $M \times K$  diagonal matrix containing the singular values  $\sigma_{1,r}, \sigma_{2,r}, \dots, \sigma_{K,r}$  sorted in decreasing order. The SVS is then defined as

$$\kappa_r = \frac{\sigma_{1,r}}{\sigma_{K,r}}, \quad (4)$$

i.e. the ratio of the largest to the smallest singular value. A large SVS indicates that at least two of the user column vectors are close to parallel and spatially separating these users will therefore be difficult, whereas a  $\kappa_r$  of one (0 decibels (dB)) represents the ideal case where all the user channel vectors are pairwise orthogonal.

In order to obtain accurate results for the SVS that solely represent the achievable spatial separation, it is important to remove path-loss differences among UEs by applying a form of normalization to the raw captured matrix, which we denote as  $\mathbf{H}_r^{\text{raw}}$ . To achieve this, the first normalization described in [25] was applied. This normalization ensures that the average energy across all  $N$  resource blocks and  $M$  antennas for a given UE in  $\mathbf{H}_r^{\text{raw}}$ , denoted as  $\mathbf{h}_{i,r}^{\text{raw}}$  for user  $i$ , is equal to one. This is achieved through

$$\mathbf{h}_{i,r}^{\text{norm}} = \frac{\sqrt{MN}}{\sqrt{\sum_{r=1}^N \|\mathbf{h}_{i,r}^{\text{raw}}\|^2}} \mathbf{h}_{i,r}^{\text{raw}} \quad (5)$$

where  $\mathbf{h}_{i,r}^{\text{norm}}$  is the  $i$ th column of the normalised channel matrix  $\mathbf{H}_r^{\text{norm}}$ . This can also be thought of as applying perfect power control.

2) *Temporal Analysis*: To evaluate the change in the multi-antenna channels under mobility, an analog of the temporal correlation function (TCF) [26] was calculated. By introducing a time dependence on the measured channels, i.e., the channel vector corresponding to user  $i$  at resource block  $r$  and at time  $t$  is denoted by  $\mathbf{h}_{i,r}^{\text{raw}}[t]$ , the TCF was defined as

$$\text{TCF}_i(\tau) = \frac{\mathbf{E}\{|\mathbf{h}_{i,r}^{\text{raw}}[t-\tau]^H \mathbf{h}_{i,r}^{\text{raw}}[t]\}|}{\mathbf{E}\{\mathbf{h}_{i,r}^{\text{raw}}[t]^H \mathbf{h}_{i,r}^{\text{raw}}[t]\}}, \quad (6)$$

where  $\mathbf{E}\{\}$  denotes the expectation operator. At a given time lag  $\tau$ , the expectation is computed according to its definition, but also by averaging over all resource blocks for better statistics.

The instantaneous IUI between two users was also evaluated, i.e. users  $i$  and  $u$  with  $u \neq i$  by the normalized expected inner product

$$\text{Int}_{i,u}^t[t] = \frac{|\mathbf{h}_{i,r}^{\text{raw}}[t]^H \mathbf{h}_{u,r}^{\text{raw}}[t]|}{\sqrt{\mathbf{h}_{i,r}^{\text{raw}}[t]^H \mathbf{h}_{i,r}^{\text{raw}}[t] \mathbf{h}_{u,r}^{\text{raw}}[t]^H \mathbf{h}_{u,r}^{\text{raw}}[t]}} \quad (7)$$



Fig. 2. User Equipments. Left: pedestrian carts. Right: car mounting.

This provides a metric to evaluate to what extent the, so-called, massive MIMO favorable propagation conditions [27] hold in a practical system.

#### D. User Equipment

As mentioned at the beginning of Sec. II, each UE is a two-channel USRP, four of which were used in these measurements to provide a total of 8 spatial streams. The USRPs were mounted in carts to emulate pedestrian behaviour and in cars for higher levels of mobility, as shown in Fig. 2. Sleeve dipole antennas were used in each case. On the carts, the dipole antennas were attached directly to both RF chains of the USRP with vertical polarisation. With a fixed spacing of  $2.6\lambda$ , these can either be considered as two devices in very close proximity or as a single, dual-antenna device. In Fig. 2, the USRPs shown in carts each have only one antenna connected. For the cars, the antennas were roof mounted with vertical polarization on either side of the car, giving a spacing of approximately 1.7 m. Each UE's RF chain operates with a different set of frequency-orthogonal pilots and synchronises over-the-air (OTA) with the BS using the primary synchronisation signal (PSS) broadcast at the start of each 10 ms frame. The PSS was transmitted using a static beam pattern and the local oscillators (LOs) of the UEs were global positioning system (GPS) disciplined to lower carrier frequency offset to improve sync stability.

### III. MEASUREMENT SCENARIO

In this section, the measurement scenario and two configurations used to obtain both static and mobile measurements are described. Both measurements can be considered as predominantly LOS with an expected channel estimation signal to noise ratio (SNR) range of approximately 20 dB to 30 dB per RF chain over the measurement runs considered.

#### A. LOS Static Configuration

To obtain a point of reference for the mobile configuration, a static trial was conducted first using the pedestrian carts. Four dual-antenna USRPs acting as 8 UEs were placed 32 m away from the BS in a parallel line where car 2 (C2) is shown in Fig. 3. The carts were well separated (approximately 2 m



Fig. 3. Overview of the measurement scenario at the campus of the Faculty of Engineering (LTH), Lund University, Sweden. Arrows indicate the direction of movement for the cars C1 and C2. Pedestrians P1 and P2 moved within the zones indicated by their white boxes.

apart), each UE transmitted with a fixed power of approximately 0 dBm, and  $Y_r, \forall r$  was recorded for 60 s. Movement was kept to a minimum within the surrounding environment during capture period.

#### B. LOS Mobile Configuration

For the mobile trial, a mixture of both pedestrian and vehicular UEs were introduced, so that it would be possible to observe how the massive MIMO channel behaves over time in a more dynamic situation. Each user again transmitted with the same fixed power level and  $Y_r, \forall r$  was captured for a 30 s period. Two pedestrian carts, indicated by P1 and P2, moved pseudo-randomly at walking pace to and from one another for the measurement duration, whilst two cars, shown as C1 and C2, followed the circular route shown. For the temporal results concerning the cars, it was ensured that the captures analysed were from a period of the scenario where the cars did not exceed our maximum  $\lambda/2$  measurement speed of 29 km/h. Over the course of the entire capture, the cars completed approximately two laps and arrived back at the starting position indicated in Fig. 3. With the cars moving in this pattern, the devices are, on average, more distributed in the azimuth, but when C1 and C2 pass in parallel to the pedestrian carts they become more clustered in a perpendicular line to the BS.

### IV. RESULTS

Results from the experiments are shown here in three stages. The SVS results are inspected first, considering the impact of azimuth and elevation dimension reductions on the spatial orthogonality. These results illustrate the range of orthogonality experienced over all sampled points in space as the devices were moved. An example of channel hardening is then shown second, along with results for correlation and IUI over time between a car UE and a pedestrian UE, providing

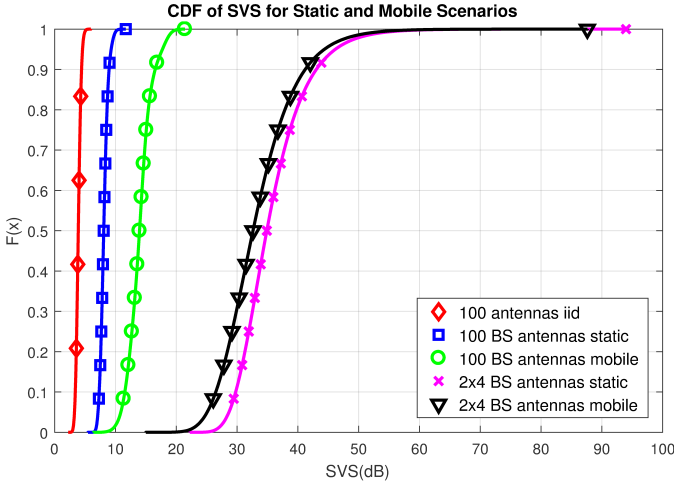


Fig. 4. CDF of SVS for static and mobile scenarios using 100 and 8 antennas at the BS.

some insight into the temporal nature of the massive MIMO channels. Finally, the uncoded UL and DL real-time BER performance is presented.

#### A. Singular Value Spread

As described in Sec. II-C1, the SVS is an effective way to study the pairwise orthogonality of the user channel vectors and thus the achievable spatial multiplexing performance for a MIMO system. The SVS results are presented here as empirical cumulative distribution function (CDF) plots for all  $N$  resource blocks and captures, i.e. across time and frequency. The result is 600,000 data points for the 30 s mobile scenario and 1,200,000 for the 60 s static scenario. The static and mobile scenario are compared first to see how much the CDF spreads out when spatial samples across the entire measurement period are considered. These results are shown in Fig. 4 for the full 100 antenna case ( $4 \times 25$ ) and an 8 antenna ( $2 \times 4$ )<sup>1</sup> case, providing the minimum for standard MU-MIMO with 8 UEs. The theoretical independent and identically distributed (iid) case for a  $100 \times 8$  system is also shown as a reference. The median value for the  $100 \times 8$  iid case here is a little over 3.8 dB with barely any variance on the CDF curve. It can be seen that the static reference measurement with 100 antennas has its median shifted from this by 4.2 dB up to 8 dB, but it also has a similar stability to the iid case with very small levels of variance. This indicates a very good level of spatial separation in LOS that is likely to be predominantly limited by the angular resolution provided by the azimuth dimension of the BS array (25 antenna elements) and the dual-UE terminals with only  $2.6\lambda$  spacing between antennas. The result may have improved if 8 single-antenna devices were served with a more reasonable spacing. With only 8 antennas at the BS, as would be the case in a standard MU-MIMO system, the median value in the static case is approximately 35 dB with an upper tail reaching out towards 94 dB. This indicates that the user vectors are highly parallel and it will

<sup>1</sup> $2 \times 4$  was chosen to provide a similar array shape and azimuth dominance to the full  $4 \times 25$ , 100 antenna case.

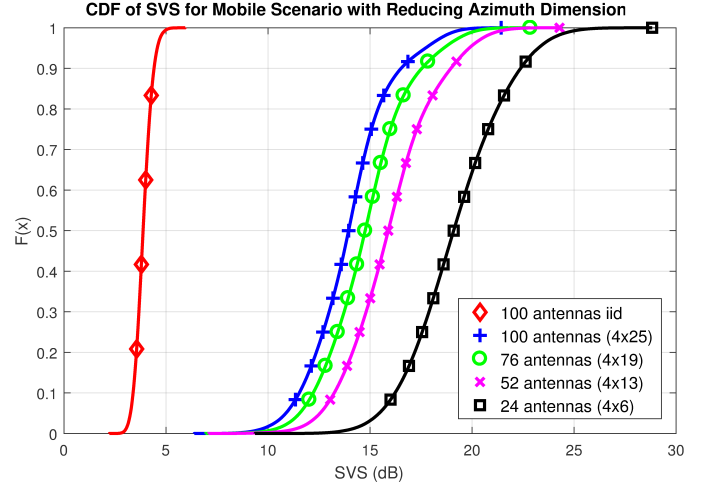


Fig. 5. CDF of SVS for mobile scenario with reducing azimuth dimension.

be far more difficult to establish reliable spatial modes. In the mobile case with 100 BS antennas the median shifts to nearly 14 dB, twice the magnitude of the static case. The best case scenario at the lower tail of the curve comes in line with the static measurement, but the variance over the measurement period has increased, reaching a peak SVS of 21 dB. However, the upper tail of the curve is still relatively small with a 90th percentile of 16.5 dB, indicating a good level of stability and a restriction in the extremity of the variations. With only 8 BS antennas, the median SVS increases to 32.5 dB, and the majority of the CDF plot up to the 41 dB 90th percentile has decreased 2.5 dB from the static case. This illustrates that with only 8 antennas, separating the static users equally spaced by approximately 2 m in a single parallel line proved more difficult than the dispersed mobility scenario. In summary, these results indicate that the variation between spatial channel magnitudes can be kept below 16.5 dB for 90% of the LOS scenario shown with an  $M$  to  $K$  ratio of 12.5.

#### B. Azimuth vs. Elevation

One topic of considerable interest for massive MIMO deployments is an optimal array configuration. Massive MIMO performance is generally expected to be higher in a cellular scenario when using a more azimuth dominant configuration due to a higher spread in the angular arrival of multipath components, but the extent to which this affects actual performance in real scenarios will help determine the compromises which can be made for a feasible deployment. In addition, when the scenario is LOS or more Rician in nature, the dominant components will become directional beams and higher performance would be expected when the array dimension is largest in the plane the UEs are spread. For example, when the UEs are placed in a line perpendicular to the BS with differing distances, one would typically prefer additional resolution in the elevation to resolve them. Fig. 5 shows the SVS for the 30 second mobile scenario as the azimuth dimension of the array is reduced in intervals of one quarter, starting

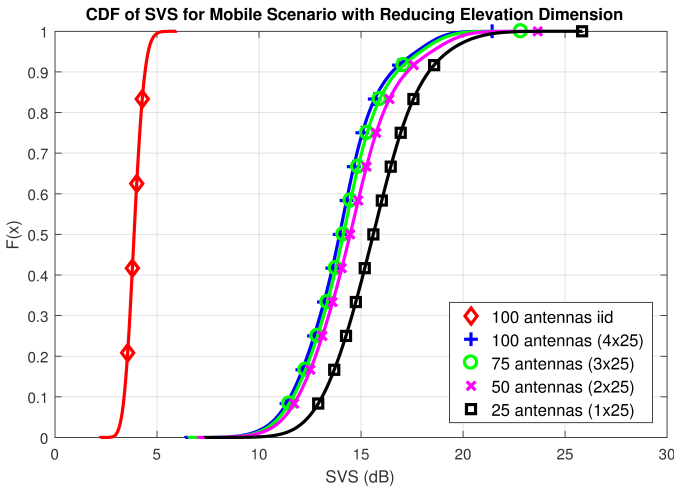


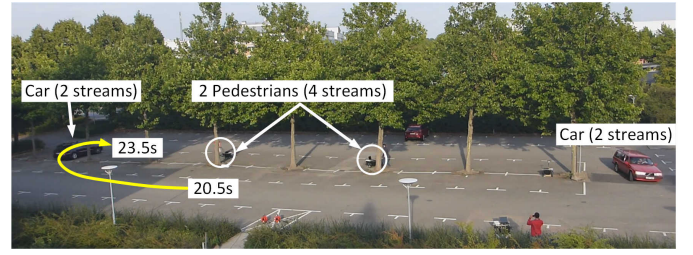
Fig. 6. CDF of SVS for mobile scenario with reducing elevation dimension.

from the outside edges and moving in<sup>2</sup>. Moving through the first 3 configurations, a clear shift of the curve by steps of approximately 1 dB can be seen and only a slight growth in the upper tail. Once the  $4 \times 6$  case is reached, the median SVS magnitude has increased by 5 dB to 19 dB. In Fig. 6 the SVS results for the same mobile scenario are shown, but this time with the elevation dimension of the array reducing by 1 row (one quarter) at a time. It is immediately apparent that the results for the first three steps do not differ significantly at all from the full 100 antenna case. The upper tail has extended by just over 1 dB, but the median and 90th percentile have increased by only 0.2 dB and 0.5 dB, respectively. As the antenna dimensions are reduced, it can be seen that all configurations are closer to the full 100 antenna curve than in the reduced azimuth cases. Even the  $1 \times 25$  case where there is no elevation resolution outperforms the  $4 \times 13$  case. This shows that for this particular scenario, there is more to gain from the azimuth dimension, and a similar level of performance could be obtained by halving the number of antennas in the elevation dimension. However, looking at the two CDF plots, one could argue that the difference is not significant enough to prefer the extended azimuth arrangement, particularly with the deployment difficulties it could introduce for mast mounting. This could be indicative that a more symmetrical arrangement such as that shown for FD-MIMO in [8] and [9] would provide sufficient performance when compared to an azimuth dominated configuration. More experiments need to be conducted in urban environments with richer scattering for both LOS and non-line-of-sight (NLOS) situations to confirm this.

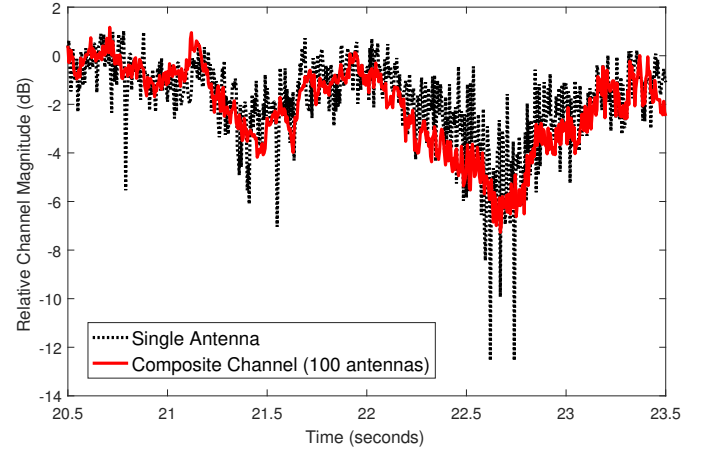
### C. Temporal Analysis

The temporal results were based on two different time periods within the 30 second mobility scenario. Channel hardening results are presented first for one car user using a 3 second period of the full 30 second capture, specifically between 20.5 s and 23.5 s. Time correlation and IUI results

<sup>2</sup>It was only possible to reduce by multiples of 2 due to the  $4 \times 25$  array configuration.



(a)



(b)

Fig. 7. Resilience to fading. a) View from BS with 3 second car-based user path indicated. b) Relative channel magnitude for both a single antenna and the composite MIMO channel to the depicted user over the 3 second period.

are then shown for a 4 second period between 10 s and 14 s where both cars travel in parallel to the BS. For both of these time periods, the vehicle speed remains below 29 km/h.

1) *Channel Hardening*: From theory, fast-fading is shown to disappear when letting the number of BS antennas go to infinity, as discussed in [1] and [2]. Whilst the measured scenarios will have been more of a Rician than Rayleigh nature due to the UEs being predominantly in LOS, it was still possible to inspect the less severe fading dips of a single channel for a single UE and evaluate them against the composite channel formed by the  $100 \times 8$  massive MIMO system. In Fig. 7a, a 3 second portion of the captured mobile scenario is shown as viewed from the BS. An arrow indicates the movement of one of the cars during this three second period. For one UE in this car over the acquisition period shown, the channel magnitude of a single, vertically polarised BS antenna was extracted, along with the respective diagonal element of the user side Gram matrix  $\mathbf{H}_r^H \mathbf{H}_r$  for one resource block  $r$ . Their magnitudes are plotted against each other in Fig. 7b after normalization. It can be seen that the composite channel tends to follow the average of the single antenna case, smoothing out the faster fading extremities, and larger variations occur over the course of seconds rather than milliseconds.

Fig. 8 shows the correlation of the signal power over time offset for a pedestrian UE and a car UE when using either one antenna or 100 antennas. Due to the channel hardening and

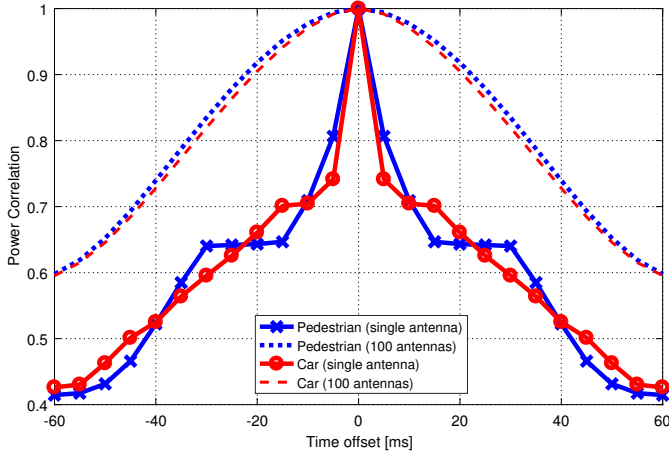


Fig. 8. Correlation of the power for signal on one antenna versus 100 antennas for a pedestrian and car UE.



Fig. 9. 4 second subset of mobility scenario (10s to 14s of full 30 second capture) used for temporal analysis. Arrows indicate the movement of each UE over the 4s duration. Car 2 does not exceed the maximum allowed speed of 29 km/h.

the constructive combining of 100 signals, the power levels are much more stable as compared to the single antenna case. For this particular case, with 100 antennas, power control can be done at least five times slower than with a single antenna. These two figures show, that performance of this nature not only demonstrates an improvement in robustness and latency due to the mitigation of fast-fade error bursts, but also that it is possible to greatly relax the update rate of power control when combining signals from many antennas.

2) *Time Correlation*: As a UE moves, it is of interest to view the correlation of the MIMO channel vectors over time in order to ascertain how quickly the channel becomes significantly different. This will play a part in determining the required channel estimation periodicity for a given level of performance. In Fig. 9, a 4s second period of the 30 second mobility scenario is shown, with the arrows indicating the movement of each UE during that period. Using one UE from Car 2, the absolute values of the time correlation function for all resource blocks over the 4 second period are shown in Fig. 10 for the first 1.5s of movement. Within the first 500ms at this speed, the level of correlation has dropped significantly in the 100 antenna case to 0.3, whilst the 8 antenna case remains above 0.8 for the entire 1.5s duration with a far shallower decay. For the 8 antenna and

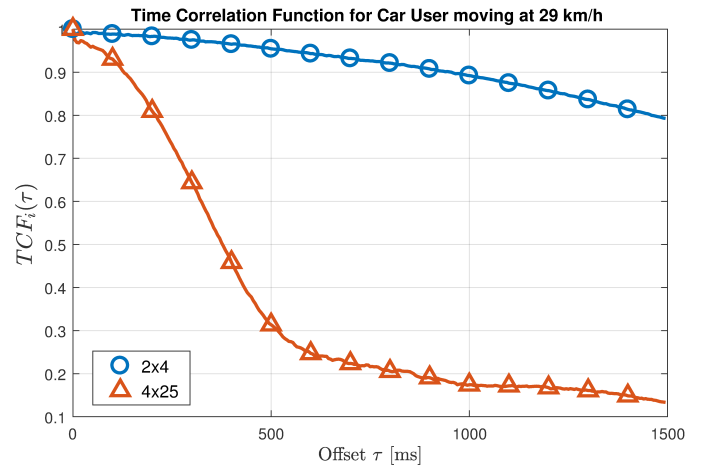


Fig. 10. Correlation of the composite channel over time for all resource blocks of car 2 at a speed of 29 km/h. 100 antenna and 8 antenna cases are shown in 4x25 and 2x4 configurations respectively. Both curves are normalized to themselves, so array gain is not visible here.

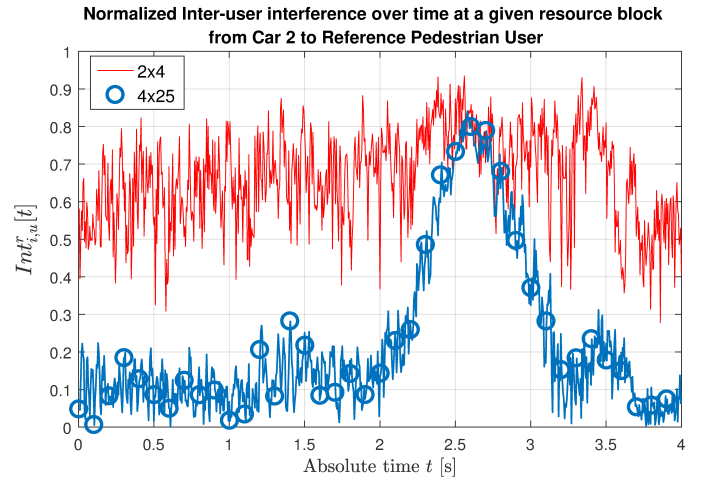


Fig. 11. IUI between car 2 and pedestrian user 1 over time

100 antenna cases to become decorrelated by 20 percent, it takes 1455 ms and 205 ms respectively; a factor difference of approximately 7. This highlights how the precise spatial focusing of energy provided by massive MIMO translates to a larger decorrelation in time from far smaller movements in space. The acceptable level of decorrelation will depend upon many factors such as the desired level of performance, the detection/precoding technique and the modulation and coding scheme (MCS), but this result provides some insight into how rapidly a real channel vector can change in massive MIMO under a moderate level of mobility.

3) *Inter-User Interference*: Using the same 4s scenario depicted in Fig. 9, the IUI for the entire period was calculated between a single UE in car 2 and a reference pedestrian, indicated as Ref in the figure. For clarity, it should be noted that IUI here is a measure of user correlation; with ZF precoding applied, the actual IUI is small in practice. In Fig. 11 the normalized IUI is shown plotted over time for both 8 and 100 antennas, and in Fig. 12 as an empirical CDF. In the

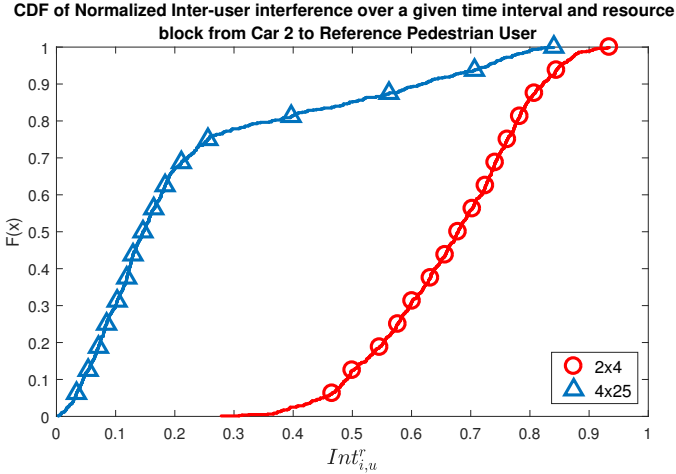


Fig. 12. CDF of interference between car 2 and pedestrian user 1

8 antenna case, the IUI median is approximately 0.7 with a large variance from 0.28 up to 0.93. At 2.5 s into the scenario period, where it can be seen that car 2 will pass close to the reference user, the IUI in Fig. 11 does not appear to increase much beyond the average it is already maintaining. In the same graph for the 100 antenna case, the median IUI is 0.15 and the level rises only significantly as the car passes close to the reference user. The level it peaks at is only a little under that of the 8 antenna case, but it rolls off to below 0.3 in approximately 500ms. This interference anomaly can be seen in the CDF of Fig. 12 as a long upper tail, but the 75th percentile remains below 0.25. These results illustrate that about a two times reduction in the median level of IUI between two users can be achieved in LOS using 100 antennas over 8, but also that a smaller elevation resolution could limit the massive MIMO benefits when users stack densely in a perpendicular line. However, it is likely that this could be mitigated further with intelligent user grouping.

#### D. Uncoded BER Performance

In addition to the UL pilot transmissions, the uncoded, real-time BERs for both the UL and DL of each spatial mode using ZF detection/precoding were recorded to provide an indication of the true system performance under mobility. As no power control or user grouping was applied, quadrature phase-shift keying (QPSK) modulation was used on each spatial stream for robustness. In Fig. 13, the BERs for pedestrian and vehicular users in the mobile scenario are plotted as separate empirical CDFs for both the UL and DL. The static scenario BERs had a 95th percentile of 0 error, with the last 5 percent coming in below  $10^{-5}$ . This is stated here for reference purposes, but omitted from the CDF plot. In first considering the UL, it can be seen that the pedestrian BER outperforms the vehicular up to the 80th percentile where both intersect at a BER of  $10^{-2}$ , but the cars appear to suffer less in the upper extremities, tailing off early to a peak BER of 7%. This can be explained by the fact that the car antennas were roof mounted, well separated and clear of obstructions, whereas the pedestrian antenna pairs were closely spaced and occasionally shadowed

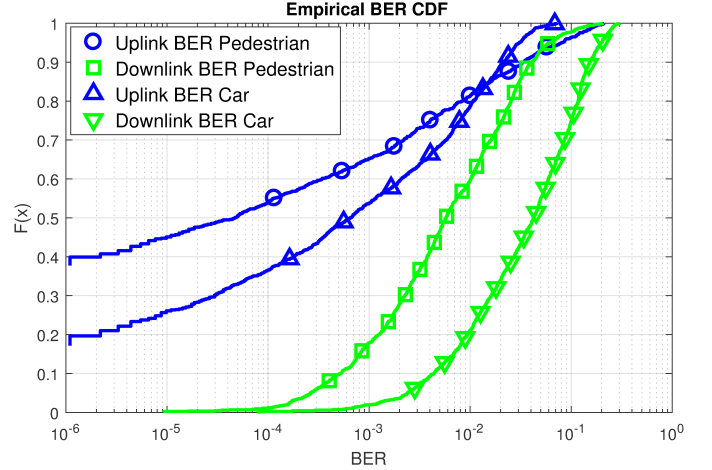


Fig. 13. CDF of uncoded BERs for static and mobile scenarios using QPSK and ZF. 0.5 ms coherence interval, mobility up to 50 km/h.

by the person pushing the cart. Thus, whilst on average the higher level of mobility provided by the cars presents a greater challenge for detection, the worst performance is experienced by the pedestrian UEs when their closely spaced USRP antennas are simultaneously shadowed. On the DL, both curves are steeper and shifted further right than the UL cases, which we would expect when both reciprocity calibration inaccuracies and channel ageing are considered. Looking at the pedestrian DL case, the upper tail appears to slightly outperform the UL. It is believed that this is because in the most extreme, shadowed cases, described above for the UL, the transmit gain of the 100 BS radios raises the terminal SNR enough for this improvement. This would also explain why, unlike the UL, the DL pedestrian BERs do not outperform the vehicular in the upper 20th percentile. These differences aside, median DL BERs of 0.5% and 4% were observed for the pedestrian and vehicular cases respectively, and 90th percentiles of 4% and 15%. Whilst the absolute SNR at each UE or BS antenna was not measured, these results still illustrate that the system was able to track the channel accurately enough to maintain 8 reliable spatial streams using under moderate mobility with no user grouping or power control. With the latter enhancements in place and an error-correcting code, it is highly likely that the system could provide satisfying performance, even with higher-order modulation schemes.

## V. CONCLUSIONS

The performance of a  $100 \times 8$  real-time massive MIMO system operating in LOS with moderate mobility has been presented and analysed. To the best of the authors' knowledge, these are the first results of their kind that begin to indicate the performance of massive MIMO as the composite channel changes over the course of a more dynamic scenario. The SVS results indicate that azimuth resolution is still to be preferred overall in a LOS situation with minimal scatters present, but the difference is perhaps not significant enough to warrant the inherent cost and complexity involved when deploying a physically long array. The IUI results also indicate that lack of elevation resolution could cause problems for users densely

bunched in a perpendicular line, but situations like this may be improved with intelligent user grouping. When considering the correlation of mobile channel vectors over time, it was shown that the 100 antenna case decorrelated by 20% 7 times faster than the 8 antenna case, providing an indication of the spatial focusing effect in a MIMO system. Finally, for the mobile scenario illustrated, it was shown that BERs of 1% and 10% for the 80th percentile can be achieved for UL and DL respectively, using QPSK with ZF and no form of power control, user grouping or error-correcting code.

#### ACKNOWLEDGMENT

The authors wish to thank all academic staff and post graduate students involved who contributed to the measurement trial operations. They also acknowledge the financial support of the Engineering and Physical Sciences Research Council (EPSRC) (EP/I028153/1), the European Union Seventh Framework Programme (FP7/2007-2013) under grant agreement no. 619086 (MAMMOET), NEC, NI, the Swedish Foundation for Strategic Research and the Strategic Research Area ELLIIT.

#### REFERENCES

- [1] T. L. Marzetta, "Noncooperative cellular wireless with unlimited Numbers of base station antennas," *IEEE Transactions on Wireless Communications*, vol. 9, no. 11, pp. 3590–3600, Nov 2010.
- [2] E. G. Larsson *et al.*, "Massive MIMO for next generation wireless systems," *IEEE Communications Magazine*, vol. 52, no. 2, pp. 186–195, February 2014.
- [3] E. Björnson, J. Hoydis, M. Kountouris *et al.*, "Massive MIMO systems with non-ideal hardware: Energy efficiency, estimation, and capacity limits," *IEEE Transactions on Information Theory*, vol. 60, no. 11, pp. 7112–7139, Nov 2014.
- [4] J. Hoydis *et al.*, "Massive MIMO in the UL/DL of cellular networks: How many antennas do we need?" *IEEE Journal on Selected Areas in Communications*, vol. 31, no. 2, pp. 160–171, feb 2013.
- [5] C. Shepard *et al.*, "Argos: practical many-antenna base stations," in *Proceedings of the 18th annual international conference on Mobile computing and networking - Mobicom '12*, no. i. ACM Press, 2012, p. 53.
- [6] C. Shepard *et al.*, "ArgosV2 : A flexible many-antenna research platform," Tech. Rep., 2013.
- [7] H. Suzuki *et al.*, "Highly spectrally efficient Ngara rural wireless broadband access demonstrator," in *2012 International Symposium on Communications and Information Technologies, ISCIT 2012*, 2012, pp. 914–919.
- [8] Y. Li, Y. Xm, M. Dong *et al.*, "Implementation of full-dimensional MIMO (FD-MIMO) in LTE," in *2013 Asilomar Conference on Signals, Systems and Computers*, Nov 2013, pp. 998–1003.
- [9] Y. H. Nam, B. L. Ng, K. Sayana *et al.*, "Full-dimension MIMO (FD-MIMO) for next generation cellular technology," *IEEE Communications Magazine*, vol. 51, no. 6, pp. 172–179, June 2013.
- [10] W. Zhang *et al.*, "Field trial and future enhancements for TDD massive MIMO networks," in *2015 IEEE 26th Annual International Symposium on Personal, Indoor, and Mobile Radio Communications (PIMRC)*, 2015.
- [11] "Facebook Project Aries," 2016. [Online]. Available: <https://code.facebook.com/posts/1072680049445290/introducing-facebook-s-new-terrestrial-connectivity-systems-terragraph-and>
- [12] J. Vieira *et al.*, "A flexible 100-antenna testbed for massive MIMO," in *Globecom Workshops (GC Wkshps)*, 2014, pp. 287–293.
- [13] "Bristol Is Open," 2014. [Online]. Available: <http://www.bristolisopen.com/>
- [14] S. Malkowsky, J. Vieira, L. Liu *et al.*, "The world's first real-time testbed for massive MIMO: Design, implementation, and validation," *IEEE Access*, submitted, 2016. [Online]. Available: <https://arxiv.org/abs/1701.01161>
- [15] P. Harris, S. Zhang, M. Beach *et al.*, "LOS Throughput Measurements in Real-Time with a 128-Antenna Massive MIMO Testbed," in *Globecom*, 2016.
- [16] P. Harris, W. B. Hasan, S. Malkowsky *et al.*, "Serving 22 Users in Real-Time with a 128-Antenna Massive MIMO Testbed," in *2016 IEEE International Workshop on Signal Processing Systems (SiPS)*, Oct 2016, pp. 266–272.
- [17] P. Kela, X. Gelabert, J. Turkka *et al.*, "Supporting mobility in 5G: A comparison between massive MIMO and continuous ultra dense networks," in *2016 IEEE International Conference on Communications (ICC)*, May 2016, pp. 1–6.
- [18] A. Papazafeiropoulos, H. Ngo, and T. Ratnarajah, "Performance of massive MIMO uplink with zero-forcing receivers under delayed channels," *IEEE Transactions on Vehicular Technology*, vol. PP, no. 99, pp. 1–1, 2016.
- [19] A. Papazafeiropoulos, "Impact of general channel aging conditions on the downlink performance of massive MIMO," *IEEE Transactions on Vehicular Technology*, vol. PP, no. 99, pp. 1–1, 2016.
- [20] "USRP-RIO 2943 datasheet," 2014. [Online]. Available: <http://www.ni.com/datasheet/pdf/en/ds-538>
- [21] J. Vieira, F. Rusek, O. Edfors *et al.*, "Reciprocity calibration for massive MIMO: Proposal, modeling and validation," *CoRR*, vol. abs/1606.05156, 2016. [Online]. Available: <http://arxiv.org/abs/1606.05156>
- [22] S. Malkowsky, J. Vieira, K. Nieman *et al.*, "Implementation of low-latency signal processing and data shuffling for TDD massive MIMO systems," in *2016 IEEE International Workshop on Signal Processing Systems (SiPS)*, Oct 2016, pp. 260–265.
- [23] D. Gesbert, M. Shafi, D. shan Shiu *et al.*, "From theory to practice: an overview of MIMO space-time coded wireless systems," *IEEE Journal on Selected Areas in Communications*, vol. 21, no. 3, pp. 281–302, Apr 2003.
- [24] A. Paulraj, R. Nabar, and D. Gore, *Introduction to space-time wireless communications*. Cambridge university press, 2003.
- [25] X. Gao *et al.*, "Massive MIMO performance evaluation based on measured propagation data," *IEEE Transactions on Wireless Communications*, vol. 14, no. 7, pp. 3899–3911, July 2015.
- [26] A. Molisch, *Wireless Communications*, ser. Wiley - IEEE. Wiley, 2010. [Online]. Available: <https://books.google.co.uk/books?id=vASyH5-jfMYC>
- [27] E. Björnson, E. G. Larsson, and T. L. Marzetta, "Massive MIMO: 10 myths and one grand question," *CoRR*, vol. abs/1503.06854, 2015. [Online]. Available: <http://arxiv.org/abs/1503.06854>



**Paul Harris** received the B.Eng. degree in Electronic Engineering from the University of Portsmouth in 2013 and joined the Communication Systems & Networks Group at the University of Bristol in the same year to commence a PhD. His research interests include massive MIMO system design, real-world performance evaluation and the optimisation of techniques or algorithms using empirical data. Working in collaboration with Lund University and National Instruments, he implemented a 128-antenna massive MIMO test system and led two research teams to set spectral efficiency world records in 2016. For this achievement, he received 7 international awards from National Instruments, Xilinx and Hewlett Packard Enterprise.



**Steffen Malkowsky** received the B.Eng. degree in Electrical Engineering and Information Technology from Pforzheim University, Germany in 2011 and the M.Sc. degree in Electronic Design from Lund University in 2013. He is currently a PhD student in the Digital ASIC group at the department of Electrical and Information Technology, Lund University. His research interests include development of reconfigurable hardware and implementation of algorithms for wireless communication with emphasis on massive MIMO. For the development of a massive MIMO testbed in collaboration with the University of Bristol and National Instruments, and a spectral efficiency world record, he received 7 international awards from National Instruments, Xilinx and Hewlett Packard Enterprise.



**Joao Vieira** received the B.Sc. degree in Electronics and Telecommunications Engineering from University of Madeira in 2011, and the M.Sc. degree in Wireless Communications from Lund University, Sweden in 2013. He is currently working towards a Ph.D. degree at the department of Electrical and Information Technology in Lund University. His main research interests regard parameter estimation and implementation issues in massive MIMO systems.



**Erik Bengtsson** received M.Sc. in Electrical Engineering from Lund University 1997. He joined Ericsson Mobile Communication AB in Lund the same year and worked with RF ASIC design until 2005. He then joined Nokia A/S in Copenhagen and worked with antenna concept development with focus on reconfigurable antennas. In 2011 he joined Sony Mobile in Lund and belongs to the Network Technology lab. From 2015 he is an industry PhD student at the Department of Electrical and Information Technology, Lund University, partly funded by

Swedish Foundation for Strategic Research (SSF). His current research focus is terminal diversity aspects from a massive MIMO perspective.



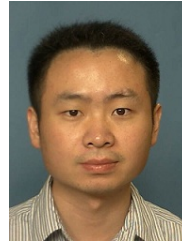
**Fredrik Tufvesson** received his Ph.D. in 2000 from Lund University in Sweden. After two years at a startup company, he joined the department of Electrical and Information Technology at Lund University, where he is now professor of radio systems. His main research interests are channel modelling, measurements and characterization for wireless communication, with applications in various areas such as massive MIMO, UWB, mm wave communication, distributed antenna systems, radio based positioning and vehicular communication. Fredrik has authored

around 60 journal papers and 120 conference papers, recently he got the Neal Shepherd Memorial Award for the best propagation paper in IEEE Transactions on Vehicular Technology.



**Wael Boukley Hasan** received his M.Sc. in Mobile Communications Engineering with distinction from Heriot-Watt University in 2013. After graduating, he worked for one year in Alcatel-Lucent in the Small Cells Platform Development Department. He then joined the CDT in Communications at the University of Bristol in 2014. His research within the CSN group is focused on investigating and developing different techniques for massive MIMO, with an interest in increasing spectral efficiency and power efficiency. He was a member of the University of

Bristol research team that set spectral efficiency world records in 2016 in collaboration with Lund University.



**Liang Liu** received his B.S. and Ph.D. degree in the Department of Electronics Engineering (2005) and Micro-electronics (2010) from Fudan University, China. In 2010, he was with Rensselaer Polytechnic Institute (RPI), USA as a visiting researcher. He joined Lund University as a Post-doc in 2010. Since 2016, he is Associate Professor at Lund University. His research interest includes wireless communication system and digital integrated circuits design. He is a board member of the IEEE Swedish SSC/CAS chapter. He is also a member of the technical committees of VLSI systems and applications and CAS for communications of the IEEE circuit and systems society.

of the IEEE circuit and systems society.



**Mark Beach** received his PhD for research addressing the application of Smart Antenna techniques to GPS from the University of Bristol in 1989, where he subsequently joined as a member of academic staff. He was promoted to Senior Lecturer in 1996, Reader in 1998 and Professor in 2003. He was Head of the Department of Electrical & Electronic Engineering from 2006 to 2010, and then spearheaded Bristol's hosting of the EPSRC Centre for Doctoral Training (CDT) in Communications. He currently manages the delivery of the CDT in

Communications, leads research in the field of enabling technologies for the delivery of 5G and beyond wireless connectivity, as well as his role as the School Research Impact Director. Mark's current research activities are delivered through the Communication Systems and Networks Group, forming a key component within Bristol's Smart Internet Lab. He has over 25 years of physical layer wireless research embracing the application of Spread Spectrum technology for cellular systems, adaptive or smart antenna for capacity and range extension in wireless networks, MIMO aided connectivity for through-put enhancement, Millimetre Wave technologies as well as flexible RF technologies for SDR modems underpins his current research portfolio.



**Simon Armour** Simon Armour received the B.Eng. degree in Electronics and Communication Engineering from the University of Bath, Bath, U.K., in 1996, and the Ph.D. degree in Electrical and Electronic Engineering from the University of Bristol, Bristol, U.K., in 2001. Since 2001, he has been a Member of Academic Staff with the University of Bristol, where, since 2007, he has been a Senior Lecturer. He has authored or co-authored over 100 papers in the field of baseband Physical layer and Medium Access Control layer techniques for wireless communications with a particular focus on OFDM, coding, MIMO, and cross-layer multiuser radio resource management strategies. He has investigated such techniques in general terms, as well as specific applications to Wireless Local Area Networks and cellular networks.

communications with a particular focus on OFDM, coding, MIMO, and cross-layer multiuser radio resource management strategies. He has investigated such techniques in general terms, as well as specific applications to Wireless Local Area Networks and cellular networks.



**Ove Edfors** is Professor of Radio Systems at the Department of Electrical and Information Technology, Lund University, Sweden. His research interests include statistical signal processing and low-complexity algorithms with applications in wireless communications. In the context of Massive MIMO, his main research focus is on how realistic propagation characteristics influence system performance and base-band processing complexity.